UCRL-86744
PREPRINT

THE BATTEL I CODE FOR SUPERCOMP

Grant H. Barkley
Thomas A. Weaver

A summary of talks presented at the IBM
Conference on Supercomputers held in Cambridge,
England, June 30 through July 10, 19 .
This paper will be published in the
Conference Proceedings which will be edited
by J. Arnett, J. Whitmer, R. Mendham,
and M. Reed

September , 19

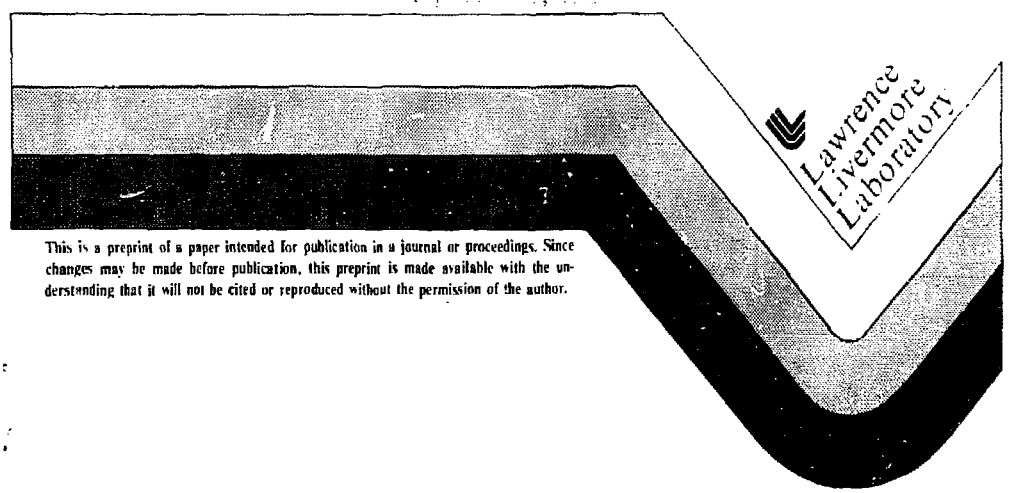

THEORETICAL MODELS FOR SUPERNOVAE

S. E. WOOSLEY

Lick Observatory, Board of Studies in Astronomy and Astrophysics,

University of California, Santa Cruz

and

Lawrence Livermore National Laboratory,

University of California

and

THOMAS A. WEAVER

Lawrence Livermore National Laboratory,

University of California

ABSTRACT

The results of recent numerical simulations of supernova explosions are presented and a variety of topics discussed. Particular emphasis is given to i) the nucleosynthesis expected from intermediate mass (10 $M_\odot$ $\leq M \leq$ 100 $M_\odot$) Type II supernovae and detonating white dwarf models for Type I supernovae, ii) a realistic estimate of the γ-line fluxes expected from this nucleosynthesis, iii) the continued evolution, in one and two dimensions, of intermediate mass stars wherein iron core collapse does not lead to a strong, mass-ejecting shock wave, and iv) the evolution and explosion of very massive stars ($M \geq 100\ M_\odot$) of both Population I and III. In one dimension, nuclear burning following a "failed" core bounce does not appear likely to lead to a supernova explosion although, in two dimensions, a combination of rotation and nuclear burning may do so. Near solar proportions of elements from neon to calcium and very brilliant optical displays may be created by "hypernovae", the explosions of stars in the mass range 100 $M_\odot$ to 300 $M_\odot$. Above ~300 $M_\odot$ a black hole is created by stellar collapse following carbon ignition. Still more massive stars may be copious producers of ^{4}He and ^{14}N prior to their collapse on the pair instability.

I. NUCLEOSYNTHESIS IN SUPERNOVAE

The study of heavy element production in supernovae has a long and distinguished history, extending back to at least 1946 when Hoyle first suggested the synthesis of a solar set of iron isotopes by the "e-process". Interestingly, the proposed ejection mechanism for this nucleosynthesis was rotation, a concept to which supernova modelers are now returning (see Section III). Since that time many people, most of whom are in attendance at this meeting, have contributed to our understanding of nuclear processes in exploding stars to the point where at least the qualitative aspects of the origin of the intermediate mass elements (carbon to nickel) are now understood. Observers too, in recent years, have found compelling evidence to support the idea that supernovae do produce heavy elements, in fact as well as in theoretical model. We refer here especially to the recent work in x-ray spectroscopy (discussed elsewhere in this volume) and the work of Kirshner and Oke (1975) and Axelrod (1980) showing evidence for freshly synthesized ^{56}Fe, and even radioactive ^{56}Co, in the spectrum of supernova 1972e.

For purposes of this workshop we shall not dwell on the historical development of nucleosynthesis theory nor on the observations, but shall instead concentrate on our own recent studies and, even so, will only summarize what has been developed in greater detail elsewhere (Weaver, Zimmerman, and Woosley 1978; Weaver and Woosley 1980; Weaver, Axelrod, and Woosley 1980; Woosley and Weaver 1980; 1981ab; Woosley, Weaver, and Tuam 1980). It now appears likely that the nucleosynthetic products of

Type I and Type II supernovae will differ markedly, a distinction that will undoubtedly have important implications for galactic chemical evolution. In general, we subscribe to the belief that Type I supernovae occur in compact, lower mass objects, such as detonating white dwarfs, and are more likely to produce heavier elements, especially iron, than are the Type II's which occur in more massive stars and are held responsible for making lighter elements such as oxygen, neon, magnesium, (perhaps) carbon, etc. This hypothesis accounts nicely for the early enhancement of [O/Fe] in our Galaxy (c.f., Clegg, Lambert, and Tomkin 1981) providing that, at early times, there existed an enhancement of massive star formation and death.

If all elements heavier than helium can be lumped together in a single group that astronomers like to call "metals", then the metallicity ejected by a star of mass $M > 13\ M_\odot$ is well fit by the expression $Z = (0.5 - 6.3 M_\odot/M)$. Multiplying this function by the mass of the exploding star gives the heavy element production in a star of mass M. If one combines this expression with an estimate of the initial mass function (e.g., Miller and Scalo 1979), which may have been time varying in the early galaxy, a value of $20 - 30\ M_\odot$ is obtained for the "representative" star such that equal amounts of heavy elements were produced in stars lighter and heavier than this mass. Of course this is a gross oversimplification of the true situation, since stars of differing mass will produce variable proportions of different heavy elements. Still, it justifies the calculation, at first pass, of nucleosynthesis in a star of $\sim 25\ M_\odot$.

The isotopic nucleosynthesis from a parametrized 25 $M_\odot$ Type II supernova (Weaver and Woosley 1980, Woosley and Weaver 1981b) is shown in Figure 1. The overproduction factor is the ratio of the mass fraction of a given species in the (homogenized) ejecta to its mass fraction in the sun (Cameron 1973). Thus a solar abundance of oxygen could have been created in the Galaxy if 1 gram out of every 14 experienced conditions similar to those characterizing the evolution of a 25 $M_\odot$ star. Dashed lines give a range of a factor of 2 for consistent production of other isotopes in solar proportions. As the figure shows, many abundant isotopes lighter than sulfur can be "properly" created in this fashion and very likely originate in intermediate mass supernovae like this one. The production of iron group species in this explosion is highly sensitive to uncertain parametrization especially the choice of the "mass cut", and the value indicated in Figure 1 may be an overestimate of the actual Type II contribution. Elements lighter than silicon are made almost entirely by pre-explosive nuclear burning and are merely pushed off of the star when it explodes. Elements heavier than silicon are produced by explosive neon, oxygen, and silicon burning. Explosive carbon burning does not occur to any appreciable extent.

There appears to be a relative deficiency of nucleosynthesis for the elements between sulfur and the iron group. Although these elements are produced with mutual proportions closely resembling those in the sun, too little mass experiences the requisite temperature range for explosive oxygen burning (3 to 4 x 10^9 K) and the absolute yield of its products is small compared to the results of other processes. The small

amount of mass heated to this range of temperature by shock wave passage is, in turn, a consequence of the steep density gradient just outside the silicon shell in the pre-explosive 25 $M_\odot$ star (Weaver, Zimmerman, and Woosley 1978, Woosley and Weaver 1981b). We have found that the pre-explosive structures of 35, 50, and 100 $M_\odot$ stars do not exhibit such a sharp decline in density around the core and, although the calculations of core bounce and explosion remain to be done in such stars, it seems likely that they may compensate for the deficient production in the $31 < A \lesssim 56$ mass range shown in Figure 1. Alternatively one may wish to consider producing most of these species in an early generation of <u>very</u> massive stars ($M \gtrsim 100\ M_\odot$, see Section IV) or by an altogether different explosion mechanism (Section III).

For lighter elements whose nucleosynthesis is not critically dependent upon explosion properties, the final abundance may be approximated by its value at the time of silicon ignition. We have evolved a variety of stellar models to the silicon ignition point. The elemental production of carbon, oxygen, and neon is summarized in Table 1 and the oxygen isotopic ratios are given in Table 2. Close agreement with solar values is encouraging and suggests that all these species have been produced in such massive stellar explosions. The slight overproduction of neon may be attributed to an uncertain solar abundance, uncertain nuclear cross-sections, especially for $^{20}Ne\ (\alpha,\gamma)^{24}Mg$, or both.

As Arnett (1971, 1973) pointed out some time ago, the neutron excess, $\eta = (N-Z)/(N+Z)$, is a critical parameter for stellar nucleosynthesis. During helium burning, this parameter is strictly determined by

the initial metallicity of the star, which is transformed into nuclei with a net neutron excess by the reaction chain $^{14}N(\alpha,\gamma)^{18}F(e^+\nu)^{18}O$. During carbon burning and subsequent stages, memory of the initial metallicity is diminished as a complex set of weak interactions increases η. The distribution of neutron excess with mass for the inner 12 $M_\odot$ of two 25 $M_\odot$ completely evolved stars is shown in Figure 2. One star, labeled Model I, had an initially solar abundance set, the other, labeled Model II, had an initial metallicity 1% as large. Memory of the distinct metallicities is clearly retained in the helium shell where the values of η differ by a factor of 100. In the carbon convective shell this difference has annealed and amounts to only a factor of 8. Still deeper within the two stars, the compositions and neutron excesses are essentially identical. This distribution of neutron excess is reflected in the final nucleosynthesis from the two stellar explosions (Table 3). Isotopes produced by hydrogen and helium burning show large variations, those from carbon and neon burning less so, and the results of oxygen burning are almost indistinguishable. Recent observations by Tomkin and Lambert (1980) of magnesium isotopic ratios in Gmb 1830, a metal deficient sub-dwarf star with an iron abundance 1/20 that of the sun, are in good accord with Table 3 ($^{25,26}Mg$ are down by a factor of 4.5 compared to ^{24}Mg). Also in good agreement are the elemental abundance determinations by Peterson (1980) for Na, Al, and Mg in a number of metal poor field stars (see Woosley and Weaver 1981b).

Important nucleosynthesis also transpires in massive stars for the very heavy elements (A > 60). The s-process in our 25 $M_\odot$ star is

similar to that studied by Lamb et al (1977) for helium burning in a another model 25 $M_\odot$ star. Additional neutron capture during carbon and neon burning increases the net neutron fluence by an additional factor of only ~ 10%. While this limited sort of s-process cannot provide the proper distribution of neutron fluxes to produce the entire solar abundance array of s-nuclei, it does move abundance peaks around and may be responsible for the production of several isotopes just above the iron group.

The p- (or γ-) process (Woosley and Howard 1978) takes place in mass shells that experience peak temperatures in the range 2.1 to 3.2 x 10^9 K, i.e., those regions that undergo explosive neon burning. In the 25 $M_\odot$ star this temperature range occurred in ~ 1 $M_\odot$ of material and, in that region, photodisintegration reactions on s-process seed should give overproduction factors ~ 260 (Woosley and Howard 1978). This implies an overproduction in the entire mass of ejected material of 260/(25 - 1.4) ~ 11, in excellent accord with the production of other, more abundant species (Figure 1). Thus massive Type II supernovae appear to properly produce the p-nuclei.

The site and nature of the r-process continues to be an unsolved problem. This is not to say that we are lacking for sites and processes that produce certain select neutron-rich nuclei. Passage of the shock wave through neon, carbon, and helium zones in a 25 $M_\odot$ star produces a limited r-process (Truran, Cowan, and Cameron 1978, Howard et al 1972), but, in the case of explosive helium burning, the amount of mass experiencing the strong neutron irradiation is too small to produce an

absolute yield of r-nuclei comparable to the abundance of s-nuclei and other heavy elements that exist in the rest of the star. Also, the neutron flux seems to be less than is required to produce a solar r-process distribution (Blake et al 1981), a difficulty that is even more extreme for explosive carbon and neon burning. An alternative site for the r-process is deeper down, near the "mass cut" that separates outgoing ejecta from the newly formed neutron star. There, material exists that is already very neutron-rich. If this material were to be completely photodisintegrated and then cooled again on a time scale short compared to that required to reassemble the heavy nuclei, a high neutron to seed ratio could be produced (Hoyle and Fowler 1960). Unfortunately this seems to require more rapid cooling than occurs in our models. We characteristically find photodisintegration products reassembling at ~ 5 x 10^9 K, too high a temperature for the r-process to proceed. Perhaps ejection by a jet (LeBlanc and Wilson 1970) could alter these results but that remains to be demonstrated. It may even be that the r-process, if indeed there is a single "r-process", does not occur predominantly in supernovae! Recent work by Cowan, Cameron, and Truran (1981) suggests that the r-process may occur during an off-center helium core flash in a low mass star (following the mixing of hydrogen into the helium core by a 2-dimensional instability). These interesting speculations point out just how uncertain the true nature of the r-process really is.

Important clues to nucleosynthesis and constraints on supernova mechanisms can often be found a single nucleus. The case of ^{48}Ca is illustrative. With an abundance 58 times that of its neighbor ^{46}Ca, it

is very difficult to produce, with any reasonable set of neutron capture cross sections, a solar abundance of ^{48}Ca without overproducing ^{46}Ca (this argument could be tightened if the capture cross sections on these two isotopes were actually measured). It is possible to produce large quantities of ^{48}Ca, however, in nuclear statistical equilibrium with a neutron excess of ~ 0.16 (Weaver, Zimmerman, and Woosley 1978). Thus it may be that the existence of such a relatively large amount of ^{48}Ca in the Galaxy requires at least the occasional ejection of some very neutron rich material. The ejection of high η material of this type may also be necessary to the origin of ^{50}Ti, ^{54}Cr, and several other rare iron-group species (Hainebach et al 1974)

Important heavy element synthesis will also occur in Type I supernovae. Currently the most successful models, (i.e., those that agree best with observation), are based upon detonating white dwarfs. Nucleosynthesis from one such typical explosion is shown in Figure 3 (Woosley, Weaver, and Taam 1980). Almost the entire mass of this 1.12 $M_\odot$ white dwarf has been converted into iron group nuclei, principally ^{56}Ni, by a passage of a detonation wave. The detailed isotopic composition remains to be computed, but should differ little from that obtained for the carbon detonation model (Arnett, Truran, and Woosley 1971), i.e., a solar abundance set for the most abundant isotopes of Cr, Mn, Fe, Co, and Ni. In the outer part of this same white dwarf, in a layer whose pre-explosive composition was nearly pure helium, explosive burning produces ^{44}Ti (Figure 3), whose later decays to ^{44}Sc and ^{44}Ca provide both a late time energy source for the supernova remnant and a pos-

sible γ-ray line signal (see Section II). Production of 1 $M_\odot$ of iron every 50 or so years by Type I explosions would provide a reasonable, although not necessarily unique, explanation for the current abundances of iron and ^{44}Ca in the Galaxy, although Ostriker (1981) has pointed out that difficulties arise if this amount of iron production in the interstellar medium has continued in recent epochs.

II. γ-LINE ASTRONOMY

As has been realized for some time, the nucleosynthesis of elemental species in novae and supernovae as radioactive progenitors provides both a late time energy source for powering the light curve and a γ-line signal that should be visible to a proper spac. or balloon-borne detector. Thus far no unambiguous signal from extra-solar radioactivity has been detected. A strong signal from positron annihilation in the vicinity of the Galactic center was discovered by balloon experiments and subsequent studies with HEAO-C found the source to be variable on a period of months. This time variability and the ability of produce positrons by methods other than radioactive decay make the connection to supernova nucleosynthesis somewhat tenuous, but the observed flux might be explained by the positrons produced during the decay of ^{56}Co made in supernovae (Clayton 1973, Woosley, Axelrod, and Weaver 1981).

Theoretical production of γ-line candidates by a 25 $M_\odot$ Type I supernovae are summarized in Table 4. About 5 times as much ^{56}Co mi[illegible]

also be produced in a Type I supernova along with a comparable abundance of ^{44}Ti (Woosley, Weaver, and Taam 1980). Given the recent optical evidence for the presence of solar mass quantities of radioactive cobalt in Type I supernova 1972e (Axelrod 1980), it is virtually certain that at least some Type I supernovae are strong γ-line emitters.

Because of the considerable uncertainty associated with the nucleosynthesis of the most important of the potential γ-line candidates in Type II supernovae (Table 4), it is useful to consider each isotope separately. The ^{56}Co and ^{57}Co production in Type II supernova is not well known since it depends on a choice for the interior mass cut (Woosley and Weaver 1981b). Radioactive tails to the light curves of such Type II explosions as 1969l suggest that at least some Type II's produce some radioactive cobalt, but others may produce none (see also Section III). The entry given in Table 4 would provide a full Galactic abundance of iron from Type II explosions (Figure 1). Another species that may be produced in both Type I and Type II supernovae is ^{44}Ti. In each case the yield is highly uncertain. In Type II's, ^{44}Ti is produced near the mass cut by very high temperature explosive silicon burning. In Type I's, production depends on the existence of a low density helium layer capping a detonating core. While this seems reasonable, there may be alternative models for Type I explosions that do not involve high temperature explosive helium burning.

The other 3 species in Table 4 should be synthesized only in Type II supernovae, supplemented in the cases of ^{22}Na and ^{26}Al, by a contribution from ordinary novae. The ^{22}Na made by supernovae comes primarily

from hydrostatic (i.e., pre-explosive) carbon burning. It is likely to be produced in all massive star explosions, but owing to its short lifetime and comparatively low yield, ^{22}Na would only be visible from a supernova in our own Galaxy, and, even then, for a relatively short time. The production of ^{60}Fe occurs as a result of the supernova shock wave passing through the helium shell and the operation of a limited r-process (Clayton 1981, Blake et al 1981). Synthesis is sensitive to shock wave energy and stellar model parameters, but production in a model 15 $M_\odot$ supernova is really quite large (Blake et al 1981). The amount given in Table 4 is approximately equal to that inferred by Clayton (1981) based on nucleosynthetic arguments and would, as he suggests, constitute a prime candidate for Galactic γ-line astronomy in the steady state.

Like ^{60}Fe, the species ^{26}Al should also accumulate in the interstellar medium from many supernovae. Woosley and Weaver (1980) [illegible] that the expected cumulative signal from Type II supernovae would be ~ 10^{-4} photons cm^{-2} s^{-1} times the present rate of Galactic heavy element production divided by the average nucleosynthesis rate over the Galactic lifetime. That is, unless the rate of element synthesis in our Galaxy has declined by more than a factor of 10 since nucleosynthesis began, the flux of ^{26}Al γ-rays, integrated over the Galactic disk, should exceed 10^{-5} photons cm^{-2}. Novae are also expected to contribute a comparable amount of ^{26}Al (Woosley and Weaver 1980, Wallace and Woosley 1981) and red giant mass loss may also be an important source (Norgaard 1980).

In addition to absolute yields, the time dependent γ-ray transparency of the expanding supernovae is critical in determining the observability of short-lived radioactivities. Woosley, Axelrod, and Weaver (1981) have carried out such an analysis for both Type I and II supernovae. Owing to their extended red giant structure and slower expansion velocities, Type II supernovae do not become transparent to their own γ-emission for about a year. The slower velocities of the heavy elements synthesized in Type II explosions ($v \sim 1000$ km s^{-1}) also implies a narrower γ-line, $\Delta E_\gamma < 10$ keV. Because they presumably lack an extended hydrogen envelope and because the heavy elements are ejected with much higher velocity ($\sim 10{,}000$ km s^{-1}) Type I supernovae become transparent to γ-rays at a much earlier time. Type I supernovae should present a strong signal of broad ($\Delta E_\gamma \sim 100$ keV) γ-lines from the decay of ^{56}Co after only several weeks of expansion. Indeed, this signal should commence shortly after maximum luminosity (Weaver, Axelrod, and Woosley 1980). Numerically, the flux from 1 $M_\odot$ of freshly synthesized ^{56}Co, normalized to a distance of 20 Mpc, would be given by

$$\phi_\gamma(^{56}\mathrm{Co}) = 4.6 \times 10^{-5}[e^{-t/114} - e^{-t/8.8}]$$

$$*(1-f_{dep})\, M_{56}\, (20\ \mathrm{Mpc}/d)^2$$

where t is the elapsed time in days since the explosion, M_{56} is the mass of radioactive ^{56}Ni initially synthesized, and f_{dep} is the time dependent γ-ray deposition efficiency (see Figure 4). Since they become transparent before ^{56}Co has substantially decayed and because they probably make more ^{56}Co to start with, Type I supernovae are much more

attractive candidates for γ-line astronomy than Type II's.

The major space mission of this decade dedicated to γ-ray astronomy is the Gamma Ray Observatory (GRO). Now scheduled for launch in 1987, this complement contains as one of its 4 experiments the Oriented Scintillation Spectrometer Experiment (OSSE) which should be an excellent tool for discovering and analyzing lines from radioactive decay. For a typical line energy of 1 MeV this experiment is capable of detecting γ-lines down to a flux of ~ 2 x 10^{-5} photons cm^{-2} s^{-1} with an observation time of roughly 1 week. Furthermore, sensitivity at least this good is maintained throughout the energy interval 100 keV to 10 MeV.

Barring the fortunate occurrence of a Galactic supernova during the 2 year lifetime of GRO, the most attractive targets of opportunity will be steady signals from ^{60}Fe, ^{26}Al, and (perhaps) ^{44}Ti within our own Galaxy, and ^{56}Co decay lines from Type I supernovae in other galaxies. Signals from ^{26}Al and ^{60}Fe, which come from Type II supernovae, should be associated with regions of active massive star formation and the Galactic disk. The ^{44}Ti signal would originate from the remnants of recent Type I and (perhaps) Type II supernovae. The strength of these emissions is highly uncertain, as we have discussed.

The sensitivity of OSSE is such that ^{56}Co emissions from as far away as the Virgo cluster (20 Mpc) should be visible from a Type I supernova producing 1 $M_\odot$ of iron. This possibility is appealing, not only because it is quite likely that at least one Type I will happen in Virgo during the course of 2 years, but also because the study of these lines would reveal interesting and unique information about the nature

of supernova and young remnants (Woosley, Axelrod, and Weaver 1981). Care must be taken, however, because the supernova rate in Virgo is not all that large. A rate of ~ 1 per year seems reasonable based on an estimated luminosity of the Virgo cluster of 2×10^{12} $L_\odot$ and a total supernova rate per year per 10^{10} $L_\odot$ of 0.008 (Tammann 1974). This is consistent with the actual discovery rate in Virgo over a 13 year search period (Tammann 1974). Perhaps this number can be doubled by including other galaxies within 20 Mpc, and maybe even multiplied by an additional factor of 2 to 5 if a relatively large fraction of nearby supernovae have gone undiscovered in the past (Tammann 1976, 1981). The point is, however, that extra-galactic γ-line astronomy can not be left to the serendipitous discovery of supernovae by OSSE. With a roughly 10 degree field of view and 10^6 s observation time, those few prime candidates may either go undetected or else decay away ($\tau_{1/2}$ = 78 d) before they are observed. We must have a ground based supernova search program operational by the time GRO goes up in 1987 (and hopefully long before that time to more properly plan observational strategy).

III. "FAILED" CORE BOUNCES IN MASSIVE STARS

Thus far our discussions of Type II supernovae have been based upon the implicit assumption that the collapse of the iron core and its subsequent rebound at nuclear density is capable of generating a strong, outgoing shock wave that will eject all material outside a mass shell of about 1.4 - 1.5 $M_\odot$. As other papers at this meeting have pointed out, this assumption is still questionable for some, if not all, masses of supernovae. (see, for example, papers by Willebrandt and by Arnett). In cases where core bounce does not lead directly to mass ejection one is left to contemplate the continued evolution of a red supergiant whose core has collapsed to a neutron star (rapidly in the process of becoming a black hole!). In the summer of 1978 we began a series of calculations to study this phenomenon. Discussions of our results were presented at the Aspen supernova workshop in 1979 and the Santa Barbara workshop in 1980. A 2-dimensional treatment of the subject is in progress by Hodenheimer and Woosley (1981) and was reviewed at the Texas Relativistic Astrophysics meeting (Woosley and Weaver 1981a).

Our study centers on a 25 $M_\odot$ star (Weaver, Zimmerman, and Woosley 1978) for which Wilson and Bowers (1978) calculated a core bounce that did <u>not</u> lead to an explosion. The trajectory of the mass shell containing 1.35 $M_\odot$ is shown in Figure 5. Here bounce occurs at 0.2495 s with t = 0 defined by the published snapshots of Weaver, Zimmerman, and Woosley (1978). The boundary of the 1.35 $M_\odot$ core initially moves outwards from a bounce radius of 1.3×10^7 cm with a velocity of $\sim 9 \times 10^8$ cm s^{-1},

reaches a maximum radius of 2.1×10^7 cm at 0.262 s, then falls back to become part of the newly formed neutron star. This motion sets up an outgoing shock in the overlying material which propagates as far as 1.50 $M_\odot$ before being overwhelmed (0.277 s) by both the inward momentum of the collapsing stellar mantle and the photodisintegration of ^{28}Si into free neutrons and protons. The velocity of inward bound material just above the dying shock is ~10,000 km s^{-1} and photodisintegration of silicon removes about 8×10^{18} erg g^{-1}. At 0.277 s, what had been an outward moving shock with positive velocity reverses sign and becomes an accretion shock. From this time on no positive velocities are observed anywhere in the calculation.

In order to see if thermonuclear burning might have an important effect in the subsequent evolution and, in particular, to see if the energy from that burning might lead to a reversal of the collapse and still create an explosion, the calculation was continued for an additional 6 s following core bounce. To facilitate the computation, the inner 1.65 $M_\odot$, which at a time 0.410 s existed in a state of near hydrostatic equilibrium, was removed from the problem and replaced by a rigid inner boundary having the same radius as that mass shell at that time, i.e., 1.007×10^7 cm. The gravitational potential of this core continued to be carried in the calculation and the removal of the core in this fashion should have little effect on the results, especially for regions outside the accretion shock. During the next 6 s, the accretion shock moved outwards in Lagrangian mass coordinate until 3.6 $M_\odot$ was contained in the neutron star core. The radial location of the shock also

moved out slowly from ~1.5 x 10^8 cm at 1 s, to ~2 x 10^8 cm [illegible], and ~4 x 10^8 cm at 6 s. Throughout this entire time the maximum accretion velocity remained very nearly constant at 10,000 km s^{-1}. Thermodynamic conditions, composition, pressure-to-gravity ratio, and Lagrangian velocity profiles are given at several times during the evolution in Figures 6, 7, 8, 9, and 10. The actual [illegible] timated in these calculations owing to the neglect of electron capture. This should have the effect of maximizing the opportunity for an explosion.

At no point during this evolution did nuclear burning lead to a velocity reversal (contrary to recent speculations by Applegate and Yahil 1981). It is important to note that the combustible mantle, which certainly contains sufficient nuclear energy to disrupt the star if it could be ignited instantaneously, does not collapse homologously (see Figure 9 for the ratio of actual pressure to that required for hydrostatic support at 2.129 s). While knowledge of core collapse is communicated to the mantle at sonic speed (roughly 5000 km s^{-1}) the pressure deficit is much greater, the density higher, and the dynamic response time therefore much shorter, for material closer to the core. The oxygen actually burns in a very thin shell ($< 0.02\ M_\odot$, Figure 8) quite close to the accretion shock. Layers farther out are supported both by the inertia of layers beneath them and by the "spherical rocket" effect of material being accelerated down into the collapsed core. An isolated layer of oxygen falling into the remnant subsonically could, in princi-

ple, reverse its infall by nuclear burning, but two effects act to inhibit this occurrence. First is the enormous pressure of the overlying star against which the burning shell must work in order to reverse its velocity. Second is photodisintegration. While oxygen burning provides about 4×10^{17} erg g^{-1} the burning of silicon to ^{54}Fe and 2 protons (the favored products in this relatively low density environment) is endoergic by 2.3×10^{16} erg g^{-1} and the photodisintegration of iron, first into free alphas, then into nucleons, removes 8.5×10^{18} erg g^{-1}. In layers immediately beneath the thin oxygen burning shell these endoergic processes rob the gas of thermal energy that might have provided support for the star (Figure 8).

In order to explore more fully the role of photodisintegration during the post-core-bounce evolution, the above calculation was repeated employing an identical parametrization except that all nuclear energy generation, both negative and positive, was suppressed once oxygen in a zone had been fully depleted. This prescription had the desired effect of suppressing thermal energy losses to photodisintegration (obviously not a realistic procedure but useful for isolating a specific effect). No explosion resulted in this case either (or at least had not resulted at a time 2.946 s when the oxygen burning shell had reached 2.7 $M_\odot$), but the evolution was clearly qualitatively different. The distinction is illustrated in Figures 11 and 12, which show velocity and thermodynamic quantities at 1.351 s, the same time as in Figures 6, 7, and 8. The accretion velocity in the model without photodisintegration is much slower at this point, by about a factor of 3, and the inner regions of

the star are not nearly so centrally condensed. Because of the shallower temperature gradient, the region where oxygen is burning is also substantially larger (~ 0.1 $M_\odot$) and there are layers, again ~ 0.1 $M_\odot$, of unburned silicon and ^{56}Ni that has not been photodisintegrated. These are all direct results of suppressing photodisintegration. Energy that would have gone into disrupting nuclei is now able to provide pressure to hold the star up in a more extended, cooler configuration. Continued evolution of this model saw the dying out of the accretion shock and a return to near hydrostatic equilibrium throughout the star. At a time of 2.95 s, no velocities greater than a few hundred km s^{-1} existed anywhere in the star. Not too surprisingly, suppressing the photodisintegration instability and ignoring electron capture makes it possible to construct a stable (at least on dynamic time scales!) stellar model in which a neutron star lies at the center of a highly evolved, supergiant star. Evolution on a thermal time scale would still be unstable due to high neutrino losses near the core.

The fact that thermonuclear burning does not appear likely to produce supernovae in 1-dimensional models with failed core bounces does not categorically remove such models from consideration since rotation is likely to be an important effect. Oxygen fuel falling almost freely towards the collapsed core will experience an increasing centrifugal barrier to its inward progress. Since rotational breaking occurs throughout a large fraction of mass concurrently and not at a single Lagrangian mass point like a shock, it is possible to stagnate large regions of unburned fuel concurrently. If inertial overshoot occurs,

then the centrifugal barrier leads to a radial bounce, and if that bounce is amplified by nuclear burning, an explosion may result. Such a mechanism is inherent in Figure 11 of Fowler and Hoyle (1964) and has been the object of recent study by Bodenheimer and Woosley (1981,BW). The essence of the BW results is that rotation plus the explosive burning of oxygen can lead, at least for some choices of parametrization, to energetic mass ejection in the equatorial plane. Details of the study, which essentially involve a 2-dimensional recalculation of the same 25 $M_\odot$ failed core bounce we have been describing, were presented at the Texas Relativistic Astrophysics meeting (Woosley and Weaver), will be the subject of a forthcoming publication (BW), and need not be duplicated here. However, the results of one such calculation are displayed in Figure 13. A steady state solution is found, displayed here at a time 15.2 s following core bounce/failure, in which matter collapsing along a radial vector roughly 60 degrees above the equatorial plane experiences a rotational bounce, accelerated by explosive oxygen burning, and then moves outwards with high velocity in the equatorial plane. At this last time step (artificially restricted by computational requirements), more than 10^{50} erg of outward directed kinetic energy is contained in about 0.5 $M_\odot$ of oxygen and oxygen burning ashes moving with a velocity of ap 5000 km s^{-1}, well above the local escape velocity. Continued evolution is likely to increase this kinetic energy as more oxygen fuel circulates and burns. A portion of this energy will be shared with the hydrogen envelope with the creation of a nearly spherical shock wave and typical Type II light curve being possible results. The asymmetric momentum of the explosion may have additional

observational consequences, however, in that the supernova remnant would retain equatorial, but not spherical symmetry. Evidence for annular structure in several remnants including SNR 1320 (Lasker 1980), 0540-69.3 (Mathewson et al. 1981), and CAS-A (Markert et al. 1981) has recently been reported. If indeed remnants like CAS-A are to be interpreted with such a model, one might anticipate (depending on the unknown interaction of the equatorially ejected oxygen blobs and the hydrogen envelope) observable differences in the spatial asymmetry of oxygen knots and hydrogen "flocculi". It would be interesting to know if such effects exist.

Since the Texas meeting several sensitivity tests have been carried out by Bodenheimer and Woosley. A calculation [illegible] lar momentum (C/G ≈ 0.06) of the one depicted also gave an explosion. The calculation that produced Figure 13 was also repeated with identical parametrization, but with all nuclear energy generation turned off. No mass ejection developed, only a stagnant accretion disk. Another calculation, which included nuclear burning but in which the inner boundary pressure was never increased (see Woosley and Weaver [illegible] to produce dynamic mass ejection. However, after an elapsed time of 41 s (11000 models of 1600 zones each!), at which time the inner core contained 6 $M_\odot$ of the original 8 $M_\odot$ carried in the problem, the remaining matter had developed a ratio of rotational energy to gravitational binding energy of 0.27 and would thus be unstable, on a dynamic time scale, to tri-axial deformation (Ostriker and Bodenheimer 1973). If a bar-like structure develops or if fragmentation ensues, angular momentum may be

transported out of the central regions of the star and may lead to mass ejection. If so, we would have come full circle to the original (Hoyle 1946) model for supernovae!

Clearly further work is greatly needed on the whole subject of "failed" core bounces. The results of Arnett and of Hillebrandt (discussed elsewhere in this same volume) have shown that if the core bounce mechanism is ever to function adequately in one dimension, it may do so only in iron cores having relatively small total mass (say $\lesssim 1.3\ M_\odot$). This is because the energy available to the shock is set, to first order, by the mass of the "homologous" core ($0.7\ M_\odot$), a quantity that is not sensitive to the total iron core mass. On the other hand, the work that the shock must do against gravity, inward momentum, and photodisintegration in order to get out of the core does increase rapidly with iron core mass. Hence larger cores are less likely to explode.

But stars of larger mass have larger cores. For example, a $25\ M_\odot$ star has a core mass of $1.61\ M_\odot$ (Weaver, Zimmerman, and Woosley 1978) while a $10\ M_\odot$ star calculated using the same physics had a core mass of $\lesssim 1.4\ M_\odot$ (Woosley, Weaver, and Taam 1980). Thus it may be that the explosion of only the lightest stars in the intermediate mass range ($10\ M_\odot$ to $100\ M_\odot$) may be attributable to core bounce of the simplest kind while the final evolution of heavier stars is sensitive to 2-dimensional effects as we have described.

It is, of course, a problem of fundamental cosmic importance to determine the critical mass [illegible] iron star remnants. If it is not too [illegible] the supernova statistics would

not be greatly altered. The lighter stars are, after all, the more abundant ones. On the other hand, our views concerning the nucleosynthesis of heavy elements would be radically altered if stars of mass greater than 25 $M_\odot$, say, do not explode by the core bounce mechanism. If this is the case, then either 2-dimensional effects such as we have just discussed, will dominate, leading perhaps to new nucleosynthetic processes involving, for example, the high temperature combustion of hydrogen and helium mixtures as the portion of the red giant envelope collapses and is equatorially expelled. Otherwise, the nucleosynthesis of intermediate mass elements may require the still more massive stars that we will now discuss.

IV. PAIR INSTABILITY SUPERNOVAE (HYPERNOVAE)

While the exact mechanism whereby stars lighter than ~ 100 $M_\odot$ become supernovae has always been controversial, the pair instability provides a straightforward explanation for explosions in more massive stars. The general nature of the instability is well understood and has been discussed elsewhere (cf. Barkat, Rakavy, and Sack 1967). The principal difficulty is, of course, that few, if any, stars this massive are believed to be currently forming. There are reasons to believe, however that more massive stars existed in the early evolution of our own and other galaxies (cf. Silk 1977), thus such stars are of interest if only for their nucleosynthesis. Also, as we shall see, the outbursts of these stars may be so energetic as to be visible to a proper (satellite-borne) detector at very great distance: perhaps even to the edge of the universe!

An important first question is the mass range for which the pair instability is likely to result in a supernova. We have evolved models of several very massive stars in order to answer this question. A 100 $M_\odot$ Pop I star studied several years ago (neglecting mass loss) evolved to silicon ignition without encountering this instability, a 150 $M_\odot$ Pop I star examined more recently, collapsed on the pair instability as it attempted to ignite carbon burning ($T_9 = 1.0$ at $\rho = 3 \times 10^4$ g cm^{-3}). We conclude that the minimum mass is somewhere between the two although mass loss on the main sequence and during helium burning could substantially increase this limit.

Since the explosion energy results solely from nuclear burning, which for these almost completely convective stars scales as M, while the gravitational binding energy scales as M^2, there also exists an upper bound to the mass of pair instability supernovae (we exclude here the very massive stars, $M > 10^5\ M_\odot$ that collapse on a general relativistic instability). This limit has also been discussed earlier by Fraley (1968) and Wheeler (1977). In order to circumvent a long calculation of envelope structure we considered, in this case, carbon-oxygen cores with ^{16}O in a 2:1 ratio to ^{12}C. Cores of 60 $M_\odot$, 80 $M_\odot$, 100 $M_\odot$ and 200 $M_\odot$ were studied. The 60, 80, and 100 $M_\odot$ cores all exploded. Nuclear burning was unable to reverse the collapse of the 200 $M_\odot$ core, and its final evolutionary state was presumably a black hole. A 150 $M_\odot$ core is currently under study in an attempt to more precisely determine the mass limit. Because of the uncertainty introduced by neglecting mass loss, relating this core size to mass on the main sequence is difficult, but we can attempt to normalize to our other models. The 150 $M_\odot$ Pop I star had a carbon-oxygen core of 93 $M_\odot$, the cores of 200 $M_\odot$ and 300 $M_\odot$ Pop III stars (to be discussed) were 103 $M_\odot$ and 370 $M_\odot$ respectively. We conclude that stars (evolving without substantial mass loss) that have main sequence masses substantially in excess of about 300 $M_\odot$ will become black holes.

Two pair instability supernovae have been studied in greater detail. One, the 150 $M_\odot$ Pop I star mentioned above is the largest mass star likely to be forming today in our Galaxy, the other, a 200 $M_\odot$ Pop III (zero metallicity) star, might have existed in the early universe

during the time (or perhaps before the time) of galaxy formation. A 500 $M_\odot$ Pop III star, whose final evolutionary state is anticipated to be a black hole, was also examined. Mass loss was neglected in these calculations for lack of a realistic prescription for its inclusion. Papaloizou (1973) and Talbot (1971) have shown that pulsational instability need not lead to substantial mass loss in these stars, thus radiatively driven winds are likely to dominate. Pulsational instabilities are automatically suppressed by the implicit nature of our hydrodynamics code which strongly damps oscillatory behavior on a time scale much shorter than the characteristic time step the code is taking. At one point we forced the time step down to 1000 s and were able to see the 150 $M_\odot$ star undergoing very small scale oscillations on the main sequence with period ~ 4.2×10^4 s. Numerical dissipation, however, precluded a further study of this phenomenon. Radiative mass loss on the main sequence was also artificially suppressed by a surface boundary pressure of 300 dyne cm^{-2} and by coarse mass zoning near the surface. Future calculations including a realistic prescription for mass loss would be interesting. At a time of 50% hydrogen depletion (1.75 my) the luminosity of the 150 $M_\odot$ star was 1.29×10^{40} erg s^{-1}, its radius, 1.8×10^{12} cm, and its effective temperature, ~ 50,000 K. By the time of hydrogen depletion ($X < 0.05$) the radius of the star had increased to 4.1×10^{14} cm, the luminosity to 1.65×10^{40} erg s^{-1}, close to the Eddington value, 2.2×10^{40} erg s^{-1} for a 150 $M_\odot$ star, and the temperature had declined to 3400 K. Given major uncertainties with regard to mass loss, these latter values and all subsequent photospheric properties are highly suspect, but there is an compellingly simple explanation

for the dramatic increase in radius (Penrod 1981). The electron scattering opacity of totally ionized helium is less than that [illegible] solar mixture of hydrogen and helium. Therefore a massive helium core has a higher Eddington limit than an equivalent sphere of solar mix. In the limit that the helium core is a large fraction of the stellar mass and radiating near its own Eddington value the luminosity in the overlying hydrogen shell will be super-Eddington. The excess radiation pressure may provoke an expansion of the envelope and rapid mass loss. Our 150 and 200 $M_\odot$ stars do not seem to have quite reached this limiting case but are close.

The age of the 150 $M_\odot$ star at hydrogen depletion was 2.[illegible] my, a value that does not vary greatly with mass for such high mass stars where luminosity and nuclear energy reservoirs both scale as M. Continued evolution saw the growth of an extended, low density ($\rho \sim 10^{-10}$ g cm^{-3}) envelope that contained an increasingly large fraction of the entire hydrogen shell. Calculations were difficult and time consuming during this stage as Lagrangian shells of small mass moved down a 10 order-of-magnitude density gradient. During this same time the surface convection region also reached down into the outer regions of the helium core mixing large quantities of helium up to the surface. At the time of helium core ignition (2.880 my, central T = 2.21 x 10^8 K, central ρ = 171 g cm^{-3}) the core contained 105 $M_\odot$ and the envelope, now all at low density, contained ~50% helium by mass. Helium burning took an additional 380,000 years and, as mentioned earlier, carbon ignition took place under unstable circumstances.

Collapsing on the pair instability, the core of the 150 $M_\odot$ star reached a maximum central temperature of 3.77×10^9 K and density of 2.02×10^6 g cm^{-3}. The nuclear energy released by explosive carbon, neon, and oxygen burning reversed this implosion giving an explosion having total kinetic energy 2.20×10^{52} erg. The resulting light curve and nucleosynthesis are shown in Figures 14 and 15 and in Table 5. Although nucleosynthesis for elements having odd Z such as Na, Al, P, Cl, and K, have not been calculated in this model, their production should also be close to solar since a Pop I set of initial seed nuclei was included and nuclear reactions during helium burning should give a "neutron excess" appropriate to their synthesis (Woosley and Weaver 1981b).

A total of $\sim 10^{51}$ erg of energy comes out in the form of electromagnetic radiation. This brilliant display, ~ 30 times brighter than a typical Type II supernova (Weaver and Woosley 1980), results both from the greater inherent energy of this massive stellar explosion and from a greater efficiency for conversion of that energy into light. During the first 8×10^6 s the luminosity comes from internal energy diffusing out through the low-density envelope. When the radius reaches 6×10^{15} cm a wave of atomic recombination begins, commencing at the surface of the star and moving inwards in both radius and mass. Radiation released by this recombination is responsible for the emissions of the next 6×10^6 s. Owing to the large volume and mass of the envelope this continues to be a very luminous phase. The decline in luminosity at about 1.4×10^7 s occurs as the transparency wave reaches the helium core boundary. This

brilliant display will be greatly diminished if the star does not retain its hydrogen envelope. The dashed line in Figure 14 shows the light output from an identical calculation in which the hydrogen envelope was artificially removed.

The evolution of the 200 $M_\odot$ Pop III star was qualitatively similar to that of the 150 $M_\odot$ Pop I star. An interesting variation, however, is the manner in which hydrogen burning in the 200 $M_\odot$ star is mediated by CNO catalyst created in the star itself prior to hydrogen ignition. The star first contracts to a temperature of 1.4×10^8 K, burns a trace of helium to create about 7×10^{-9} by mass CNO, and then commences hydrogen burning by the ordinary (not ν-limited) CNO-cycle (see also Ezer and Cameron 1971). Near the time of hydrogen exhaustion, the CNO mass fraction had grown [illegible] hydrogen exhaustion. At a time of 1/2 hydrogen depletion, the star had central temperature 1.22×10^8, density $\rho = 22$ g cm^{-3}, luminosity 2.0×10^{40} erg s^{-1}, radius 8.8×10^{11} cm, and effective temperature 7.8×10^4 K. Again the surface properties are highly uncertain owing to the neglect of mass loss. Hydrogen was depleted at an age of 2.74 my and this star too developed a highly extended structure ($R = 5.1 \times 10^{14}$ cm at helium ignition) with a helium core mass of 140 $M_\odot$ and the remainder of the star in a low density envelope of less than about 10^{-10} g cm^{-3}. As helium burning progressed, the surface convective shell ate into this core reducing its mass to ~ 105 $M_\odot$ by the end of helium burning. This convective dredge-up also increased the helium abundance in the envelope to ~ 60% (the exact value again depending on uncertain mass loss parame-

ters). At the carbon ignition stage, the star collapsed on the pair instability reaching peak temperature and density before velocity reversal of 3.88 x 10^9 K and 2.15 x 10^6 g cm^{-3} respectively. The thermodynamic conditions and collapse velocity profile at this time are shown in Figures 16 and 17. We note that for peak temperatures only slightly larger than this (i.e., T > 4.0 x 10^9) the onset of endoergic nuclear reactions would have led to a continuing collapse. Thus 200 $M_\odot$ is not far below the most massive possible pair instability supernova. The resulting explosion here produced total kinetic energy (at infinity) of 2.62 x 10^{52} erg and a light curve, effective temperature history, nucleosynthesis, and final velocity profile as given in Figures 18, 19, 20, and 21 and in Table 5. Once again this exceptionally brilliant display (~ 10^{51} erg) is critically dependent on the star retaining at least a fraction of its low density hydrogen-helium envelope up to the time of its explosion. The nucleosynthetic yield of odd Z elements, although not yet calculated for nuclei heavier than ^{14}N, should be very low owing to the lack of any heavy seed nuclei in the initial abundance set and the fact that the star collapsed without undergoing a stable stage of hydrostatic carbon burning to create the necessary neutron excess required for odd-Z synthesis (Woosley and Weaver 1981b). It is also interesting that the nucleosynthetic yield calculated here for even Z elements in the carbon to uranium range is in better accord with solar ratios than obtained by Arnett (1978) for a similar 200 $M_\odot$ helium core explosion. The difference presumably reflects a more realistic treatment of nuclear physics and time-dependent convection in the present calculation.

A 500 $M_\odot$ Pop III star is also currently under study and has been evolved through core hydrogen and (most of) core helium burning. At a time of 1/2 hydrogen depletion (age 1.1 my), the central temperature and density were 1.262 x 10^8 K and 13.8 g cm^{-3}, the central CNO mass fraction created by helium burning, 9.3 x 10^{-9}, luminosity, 6.02 x 10^{40} erg s^{-1}, radius, 1.6 x 10^{12} cm, and effective emission temperature, 76,000 K. Once again, pulsations are damped by the implicit nature of the hydrodynamics code and radiative mass loss suppressed by an artificial surface boundary pressure (500 dyne cm^{-2}) and later on, during core helium burning, by an artificial surface boundary temperature (25,000 K), to inhibit any radiation envelope formation. The artificial nature of the surface boundary conditions makes all but the central properties of this star highly suspect.

This particular 500 $M_\odot$ star is of special interest because of its ability to produce large amounts of primary nitrogen (^{14}N) in a Pop III object. The nitrogen is produced during the core helium burning phase as an extensively convective hydrogen burning shell dredges up the outer regions of a helium convective core where about 1%, by mass, carbon has been produced (although at no time is there ever a complete convective link-up between hydrogen shell and helium core). The principal thermodynamic distinction of this star appears to be the lack of a steep density gradient separating the core from the "red-giant" envelope. The entropy gradient between core and envelope is also rather shallow, about a factor of 2. At the onset of the convective dredge up phase, the helium core mass is about 300 $M_\odot$ and almost completely convective. In the steady state at the hydrogen-helium/carbon interface, hydrogen burning produces a locally super-Eddington luminosity due to both the high

[illegible]

2%, oxygen, 3%, and nitrogen, 23%. Some 290,000 years later, hydrogen is (re-)depleted in the inner 400 $M_\odot$ and, about 300,000 years after that, the $^{14}N(\alpha,\gamma)^{18}F$ reaction ignites, eventually converting all nitrogen in the inner 370 $M_\odot$ into ^{22}Ne (making a very neutron-rich core) and finally helium burns to carbon and oxygen. A residual abundance of ~20% ^{14}N and 70% ^4He remains in the outer envelope where it could be lost to a radiative wind (providing that envelope did not long ago disperse). The carbon-oxygen core itself will certainly become a black hole.

[illegible], [illegible]

regarded as [illegible] preliminary. [illegible] may rightfully be expressed [illegible] the [illegible], the artificial parametrization of surface boundary pressure and temperature, and the treatment of [illegible]. The very interesting results of these studies warrant further detailed investigations with approximate, but realistic [illegible].

This research has been supported in part by the National Science Foundation ([illegible]) and the Department of Energy ([illegible]).

REFERENCES

Applegate, J., and Yahil, A. 1981, preprint, see also this volume.

Arnett, W. D. 1971, Ap. J., 166, 153.

_____ . 1973, Ann. Rev. Astron. Ap., 11, 73.

_____ . 197[illegible]

Arnett, W. D., Truran, J. W., and Woosley, S. E. 1971, ap. J., 165, 87.

Axelrod, T. A. 1980, PhD thesis, Univ. Calif. Santa Cruz and Proc. Texas Workshop On Type I Supernovae, ed. J. C. Wheeler, Univ. Texas Press, 80.

Barkat, Z., Rakavy, G., and Sack N. 1967, Phys. Rev. Lettr., 18, 379.

Blake, J. B., Woosley, S. E., Weaver, T. A., and Schramm, D. N. 1981, Ap. J., in press.

Bodenheimer, P. and Woosley, S. E. 1981, Bull. Am. Astron. Soc., 12, 833 and in preparation for Ap. J..

Cameron, A. G. W. 1973, Space. Sci. Rev., 15, 121.

Clayton, D. D. 1973, Nat. Phys. Sci., 224, 137.

_____ . 1981, in Essays On Nuclear Astrophysics, ed. C. A. Barnes, D. D. Clayton, and D. N. Schramm (Cambridge Univ. Press).

Clegg, R. E. S., Lambert, D. L., and Tomkin, J. 1981, preprint, submitted to ap. J..

Cowan, J. J., Cameron, A. G. W., and Truran, J. W., 1981, Ap. J., in press.

Ezer, D., and Cameron, A. G. W. 1971, Ap. and Space. Sci., 14, 399.

Fowler, W. A. and Hoyle, F. 1964, Ap. J. Suppl., No. 91, 9, 201.

Fraley, G. S. 1968, Ap. and Space. Sci., 2, 96.

Hainebach, K. L., Clayton, D. D., Arnett, W. D., and Woosley, S. E. 1974, Ap. J., 193, 157.

Howard, W. M., Arnett, W. D., Clayton, D. D., and Woosley, S. E. 1972, Ap. J., 175, 201.

Hoyle, F. 1946, MNRAS, 106, 343.

Hoyle, F. and Fowler, W. A. 1960, Ap. J., 132, 565.

Kirshner, R. P., and Oke, J. B. 1975, Ap. J., 200, 574.

Lamb, S. A., Howard, W. M., Truran, J. W., and Iben, I. 1977, Ap. J., 217, 213.

Lasher, B. M. 1980, Ap. J., 237, 765.

LeBlanc, J. M., and Wilson, J. R. 1970, Ap. J., 161, 541.

Markert, T. H., Canizares, C. R., Clark, G. W., and Winkler, P. F. 1981, Bull. Am. Astron. Soc., 12, 799.

Mathewson, D. S., Dopita, L. R., Tuohy, I. R., and Ford, V. L. 1981, Ap. J., 242, L73.

Miller, G. E., and Scalo, J. M. 1979, Ap. J. Suppl., 41, 513.

Norgaard, H. 1980, Ap. J., 236, 895.

Ostriker, J. P. 1981, private communication.

Ostriker, J. P., and Bodenheimer, P. 1973, Ap. J., 180, 171.

Papaloizou, J. C. B. 1973, MNRAS, 162, 169.

Penrod, D. 1981, private communication.

Peterson, R. 1981, Ap. J., 244, 989.

Silk, J. 1977, Ap. J., 211, 638.

Talbot, R. J. 1971, Ap. J., 165, 121.

Tarmann, G. 1974, in Supernovae and Their Remnants, ed. C. B. Cosmovici, (D. Reidel : Dordrect), 155.

_____ . 1976, Proc. DUMAND Summer Workshop, ed. A. Roberts, Office of Publications, Fermi National Laboratory, 137.

_____ . 1981, private communication. see also this volume.

Tomkin, J., and Lambert, D. L. 1980, Ap. J., 235, 925.

Truran, J. W., Cowan, J. J., and Cameron, A. G. W. 1978, Ap. J., 222, L63.

Wallace, R. K., and Woosley, S. E. 1981, Ap. J. Suppl., 45, 389.

Weaver, T. A., Zimmerman, G., and Woosley, S. E. 1978, Ap. J., 225, 1021.

Weaver, T. A., and Woosley, S. E. 1980, Ann. N. Y. Acad. Sci., 336, 335.

Weaver, T. A., Axelrod, T. S., and Woosley, S. E. 1980, Proc. Texas Workshop on Type I Supernovae, ed. J. C. Wheeler, Univ. Texas Press, 113.

Wheeler, J. C. 1977, Ap. Spac. Sci., 50, 125.

Wilson, J. R., and Bowers, R. 1978, private communication.

Woosley, S. E., and Weaver, T. A. 1980, Ap. J., 238, 1017.

_____ . 1981a, Proc. 10th Texas Symp. on Relativistic Ap., to be published by the N. Y. Acad. of Sci.

_____ . 1981b, in Essays On Nuclear Astrophysics, ed. C. A. Barnes, D. D. Clayton, and D. N. Schramm, (Camb. Univ. Press).

Woosley, S. E., Weaver, T. A., and Taam, R. E. 1980, in Proc. Texas Workshop on Type I Supernovae, ed. J. C. Wheeler, Univ. Texas Press, 96.

Woosley, S. E., Axelrod, T. S., and Weaver, T. A. 1981, Comm. Nucl. and Part. Phys., in press.

Woosley, S. E., and Howard, W. M. 1978, Ap. J. Suppl., 36, 285.

TABLE 1

C, NE, AND O PRODUCTION IN MASSIVE STARS

Mass	Solar	15 $M_\odot$	20 $M_\odot$	25 $M_\odot$	35 $M_\odot$	25 $M_\odot$
Pop	Abundance	I	I	I	I	II
^{12}C	0.41	0.38	0.42	0.27	0.39	0.45
^{16}O	1	1	1	1	1	1
^{20}Ne	0.18	1.0	0.86	0.58	0.51	0.52
OV (^{16}O)		3.9	9.0	14	21	12

TABLE 2

OXYGEN ISOTOPE PRODUCTION IN MASSIVE STARS

Mass	Solar	15 $M_\odot$	25 $M_\odot$	35 $M_\odot$	25 $M_\odot$
Pop		I	I	I	II
^{16}O	8.3(-3)	0.032	0.10	0.17	0.10
$10^4(^{17}O/^{16}O)$	4.0	9.2	2.5	1.1	0.019
$10^3(^{18}O/^{16}O)$	2.3	3.1	2.1	0.61	0.028

TABLE 3

VARIATION OF NUCLEOSYNTHESIS[a] WITH STELLAR POPULATION

Species	Z = 1.7(-2)	Z = 1.7(-4)	Species	Z = 1.7(-2)	Z = 1.7(-4)
^{1}H	0.51	0.52	^{23}Na	57.4	17.9
^{4}He	1.21	1.30	^{24}Mg	22.7	15.5
^{12}C	9.1	12.7	^{25}Mg	21.6	1.7
^{13}C	0.9	0.008	^{26}Mg	25.0	2.0
^{14}N	2.6	0.033	^{27}Al	32.4	3.2
^{15}N	0.4	0.005	^{28}Si	13.3	9.3
^{16}O	14.1	11.3	^{29}Si	5.8	0.42
^{17}O	9.8	0.058	^{30}Si	6.5	0.38
^{18}O	14.9	0.15	^{31}P	8.5	1.1
^{19}F	0.8	0.008	^{32}S	7.0	3.2
^{20}Ne	37.4	33.4	^{33}S	5.7	1.7
^{21}Ne	16.5	4.0	^{34}S	10.1	6.3
^{22}Ne	7.7	0.20	^{36}S	32.6	0.20

[a]Productions are for 25 $M_{\odot}$ stars with results given as an overproduction factor relative to solar values.

TABLE 4

γ-RADIOACTIVITIES FROM TYPE II SUPERNOVAE

Species	$\tau_{1/2}$ (yr)	Mass Ejected[a] ($M_\odot$)	Synthesis Process	Years visible at 10 kpc ($\phi > 2 \times 10^{-5}$ cm^{-2} s^{-1})
^{56}Co	2.16(-1)	< 2(-1)	Exp. Si Burn	< 5
^{57}Co	7.42(-1)	< 1(-2)	Exp. Si Burn	< 10
^{22}Na	2.60(0)	3(-5)	C-Burn	15
^{44}Ti	4.7(1)	< 1(-4)	NSE	< 120
^{60}Fe	3.0(5)	< 2(-5)	Exp. Ne Burn	Continuous[b]
^{26}Al	7.2(5)	2(-5)	Exp. Ne Burn	Continuous[b]

[a]All productions except ^{60}Fe are for a 25 $M_\odot$ supernova. ^{60}Fe production is in a 15 $M_\odot$ supernova.

[b]Strength depends on present rate of nucleosynthesis in the Galaxy.

TABLE 5

NUCLEOSYNTHESIS IN PAIR INSTABILITY SUPERNOVAE[a]

Species	^{4}He	^{12}C	^{14}N	^{16}O[b]	^{20}Ne
150 $M_\odot$ Pop I	1.6(2)	0.24	5.2(-2)	1.0	0.28
200 $M_\odot$ Pop III	2.8(-2)	0.48	2.8(-3)	1.0	0.36

Species	^{24}Mg	^{28}Si	^{32}S	^{36}Ar	^{40}Ca
150 $M_\odot$ Pop I	0.96	4.1	2.6	1.3	1.5
200 $M_\odot$ Pop III	1.5	4.0	2.8	1.4	1.9

[a]Entries are ratios to solar abundances normalized to ^{16}O

[b]The ejected mass fraction of ^{16}O was 0.43 in both cases

FIGURE CAPTIONS

Fig. 1. - Final abundances from a parameterized 25 $M_\odot$, Pop. I supernova explosion having 10^{51} erg of kinetic energy, are shown compared to solar values (Cameron 1973). Dashed lines indicate a range of a factor of 2 about a consistent average overproduction factor of 14. Nuclei below sulfur appear to be produced in reasonable proportions to account for their present Galactic abunances, but the relative deficiency of element production in the range S to Mn is indicative of substantial nucleosynthesis in stars more massive than 25 $M_\odot$.

Fig. 2. - The neutron excess parameter, $\eta = \sum (N_i - Z_i) X_i / A_i$, as a function of La Grangian mass coordinate is shown for two 25 $M_\odot$ stars, one of which commenced its life with a solar (Pop. I) set of trace elements, the other with a set 1/3 as great (Pop. II). Cumulative effects of hydrostatic neutronization have led to quite similar values of η in the inner 1.5 $M_\odot$ of the two stars although substantial differences still exist in the mantles, especially in the region exterior to the carbon burning convective shell. This figure is prepared just as the maximum collapse velocity in both iron cores reaches 1000 km s^{-1}.

Fig. 3. - Nucleosynthesis in the outer layers of a detonating white dwarf model for a Type I supernova. The abundance of various species are given by mass fraction and the bottom mass scale is the mass exterior to the given La Grangian mass shell. The upper scale is ejection velocity in units of 10,000 km s^{-1}. Most of the (totally disrupted) white dwarf now consists of rapidly expanding, radioactive ^{56}Ni with a thin layer of ^{4}He on top. Other heavy elements shown are from explosive helium burning. The ^{44}Ti shown may be the source in nature of its stable daughter, ^{44}Ca.

FIGURE CAPTIONS - continued

Fig. 4. - Deposition and escape factors and lag time for a Type I supernova based on white dwarf detonation and radioactive energy input. f_{esc} is the fraction of deposited energy from radioactive decay that avoids adiabatic decompression to escape as optical or near optical emission; f_{dep} is the fraction of radioactive decay energy deposited locally (a lower bound is 0.04); and τ_e is the mean time between energy deposition and escape (or decompression). The optical luminosity is given by $L(t) = M_{56} \dot{S}(t-\tau_e) f_{dep}(t-\tau_e) f_{esc}(t-\tau_e)$ where M_{56} is the mass of radioactive ^{56}Ni produced and $\dot{S}$ is the energy production rate from ^{56}Co and ^{56}Ni decay. The γ-ray flux will be proportional to the quantity $[1-f_{dep}(t)]$. See Weaver, Axelrod, and Woosley (1978).

Fig. 5. - Radial history of that Lagrangian mass point that encloses 1.4 $M_\odot$ in a supernova core collapse calculation that did not produce a strong outward shock wave. Taken from a study by Wilson and Bowers (1978) of a 25 $M_\odot$ pre-supernova star evolved by Weaver, Zimmerman, and Woosley (1978).

Fig. 6. - Temperature, density, and radius in the interior of a 15 $M_\odot$ star at a time 1.65 s following core collapse, or 1.61 s following core bounce. The cube of the temperature has been plotted on a logarithmic scale to match the density so that the curves are parallel when the adiabatic index γ is constant and close to 4/3. The inner 1.65 $M_\odot$ has been removed from the problem and replaced by a hard boundary condition at 1.007×10^7 cm.

Fig. 7. - Same as Fig. 6, but plotted on a logarithmic radial scale. The location of the oxygen burning shell and region where iron from oxygen and silicon burning undergoes photodisintegration are indicated. The non-adiabatic cooling from photodisintegration is apparent.

Fig. 8. - Composition of the accreting and accreted material at the time corresponding to Fig. 6 and 7 (see also Fig. 10). The thin nature of the oxygen burning shell is readily apparent. Large oscillations in the abundances of free nucleons are amplifications of small temperature fluctuations that result from the artificial viscous damping of small core oscillations induced by the accreting matter.

Fig. 9. - The ratio of pressure force to gravitational force as a function of La Grangian mass coordinate at a time 2.129 s following core collapse. The units of pressure and gravity have been normalized in such a way as to give a ratio of unity if the given mass shell is in a state of hydrostatic equilibrium. The sharp spike at 2.47 $M_\odot$ is the accretion shock and the fluctuations just above are numerical (owing to a very low value of artificial viscosity employed in the calculation). The region above 4.0 $M_\odot$ (not shown) is still near hydrostatic equilibrium and has not yet responded to core collapse. The "bump" around 1.1 $M_\odot$ results from relatively coarse zoning in the pre-explosive star prior to the fine rezoning indicated in the figure.

Fig. 10. - Velocity profiles in units of 1000 km s^{-1} as a function of La Grangian mass at several times after core bounce. The slight decrease with time of the maximum infall velocity is a result of the increasing radial size of the hot shocked core. Had electron capture been properly included (it was in fact ignored in this calculation) the core would not have grown so large, thus this figure overestimates the effect. The irregular shape at the latest time indicated (6.17 s) is an artifact of coarse zoning.

Fig. 11. - Same as Fig. 6 but photodisintegration has been artificially suppressed in the shock and compressively heated matter. Comparison with Fig. [illegible] at this time a more highly extended and less centrally condensed photodisintegration is neglected.

Fig. 12. - Velocity profile corresponding to Fig. 11. Motions at this point are just becoming sub-sonic. Compare to Fig. 10.

Fig. 13. - Density profiles and velocity fields from a two-dimensional study (Bodenheimer and Woosley 1981) of a rotating 25 $M_\odot$ presupernova star whose core has collapsed without generating a strong outgoing shock (see also Fig. 5). Logarithmic density profiles are given 10 per decade. The outermost contour shown has a density of 10^5 g cm^{-3} and the innermost, 2×10^7 g cm^{-3}. A standard velocity arrow of length 1000 km s^{-1} is also indicated. At this time the polar regions have been essentially evacuated. The entire stellar mantle exists as a rapidly rotating accretion disk. A persistent velocity field has been set up involving collapse along a roughly 45° angle, nuclear burning coupled with a rotational bounce near the core, and high velocity equatorial mass ejection. The solid line in the right-hand figure is the contour of one-half oxygen depletion. Underneath and to the right of this line, the composition is that resulting from explosive oxygen burning. Above the line oxygen has not burned. The interaction of the equatorially ejected matter with the red giant envelope and the subsequent light curve remain to be calculated.

Fig. 14. - Bolometric light curve for a 150 $M_\odot$ hypernova. The solid curve is obtained if the star retains (a large fraction of) its low density hydrogen envelope. The dashed curve results if it has lost its envelope. The turnover at 140 days occurs as the transparency wave reaches the helium core - hydrogen envelope interface. The bump at 85 days is artificial (due to coarse surface zoning)

but indicates the changeover from a diffusion dominated light curve to a transparency wave. The solid line is about 30 times brighter than a typical Type II supernova.

Fig. 15. - Final nucleosynthesis from a 150 $M_\odot$ Pop. I hypernova. Products of explosive oxygen burning plus a trace of ^{56}Ni from explosive silicon burning are visible in the inner regions. The gradual slopes of the lines result both from the gradient in peak explosion temperature experienced by various mass shells and time-dependent convection, which was employed throughout the collapse and explosion phases. Material external to 120 $M_\odot$ was not carried in the core nucleosynthesis calculation, but is expected to have a composition similar to that indicated at 120 $M_\odot$.

Fig. 16. - Pre-collapse temperature and density of a 200 $M_\odot$ Pop. III (pure hydrogen-helium) star. Note the centrally condensed core and low density hydrogen-helium envelope. An adiabatic exponent close to 4/3 is apparent throughout the star leading to parallel curves for ρ and T^3.

Fig. 17. - Velocity profile at a time when oxygen first begins to burn explosively in a collapsing 200 $M_\odot$ Pop. III star. At this time the central temperature is 3.3×10^9K and density 1.3×10^6 g cm^{-3}. The low density hydrogen envelope does not participate in this collapse.

Fig. 18. Bolometric curve for a 200 $M_\odot$ Pop. III hypernova that retains its low density hydrogen-helium envelope. A spike, due to shock break out, a diffusion tail, a plateau phase as a transparency (recombination) wave eats into the envelope, and a sharp decline as that wave reaches the core-envelope interface (see Fig. 16) are all apparent features. See Fig. 14 for likely modifications if the hydrogen envelope is lost.

Fig. 19. - Effective emission temperature corresponding to Fig. 18. The same evolutionary stages are apparent.

Fig. 20. - Final velocity profile for a "200 $M_\odot$" hypernova. The outer 25 $M_\odot$ was removed prior to the completion of the calculation due to numerical difficulties associated with the low density outer layers and the artificial handling of surface boundary conditions. The sharp increase in velocity at 175 $M_\odot$ therefore corresponds to the new "surface" of the star and shock wave steepening is apparent. The final kinetic energy in this explosion was 2.62×10^{52} erg.

Fig. 21. - Nucleosynthesis from a 200 $M_\odot$ Pop. III hypernova. Products of explosive oxygen and silicon burning can be seen in the inner core. This calculation differs from that shown in Fig. 15 in that numerical difficulties precluded the inclusion of convection throughout the collapse and explosion phases. Hence the curves are not as smooth. The bulk nucleosynthetic yields and explosion energetics should not be overly sensitive to this deletion. Also convection in a medium moving at a fraction of sonic velocity is a highly questionable proposition.

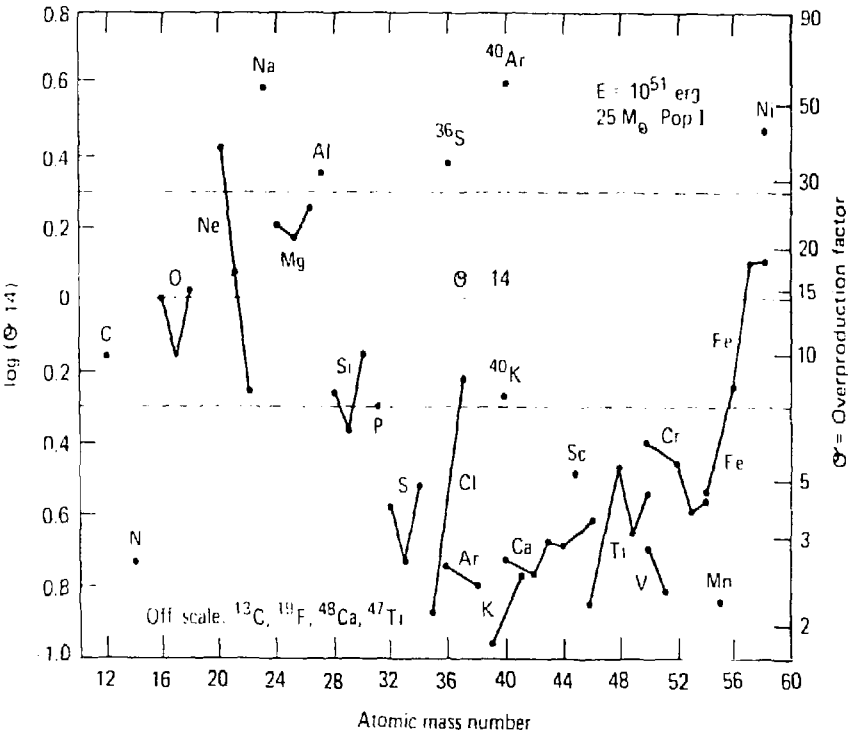
E = 10^51 erg
25 M⊙ Pop I
Off scale: 13C, 19F, 48Ca, 47Ti
log (Θ 14)
Θ = Overproduction factor
Atomic mass number
Θ 14
C
N
O
Ne
Na
Mg
Al
Si
P
S
Cl
Ar
K
36S
40Ar
40K
Ca
Sc
Ti
V
Cr
Mn
Fe
Ni

Figure 1

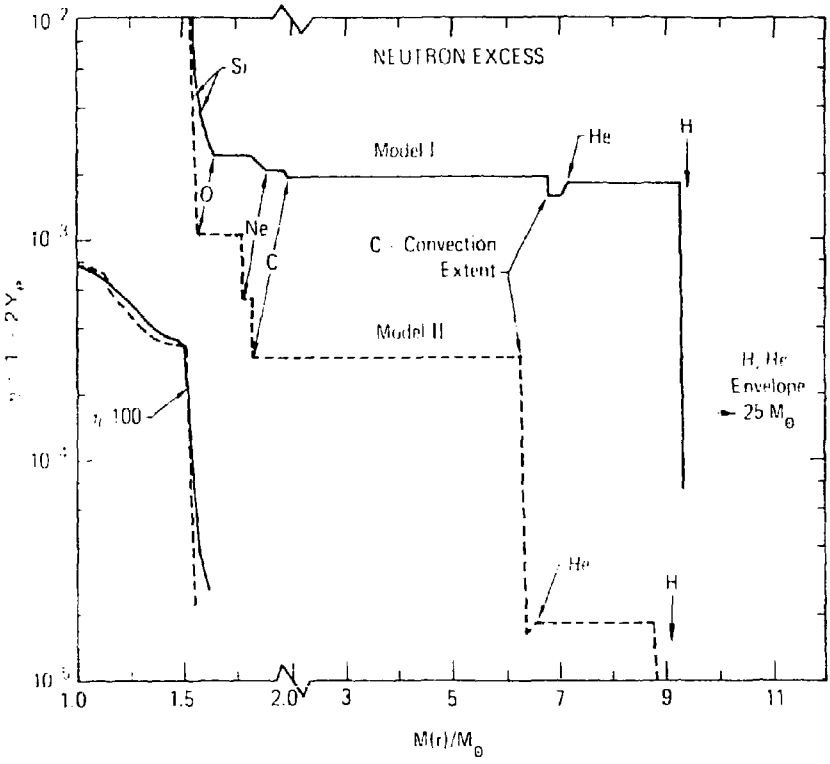
NEUTRON EXCESS
Si
O
Ne
C
Model I
He
H
C - Convection Extent
Model II
H, He Envelope ← 25 M⊙
η 100
He
H
10 2
10 3
10 4
10 5
1.0
1.5
2.0
3
5
7
9
11
M(r)/M⊙

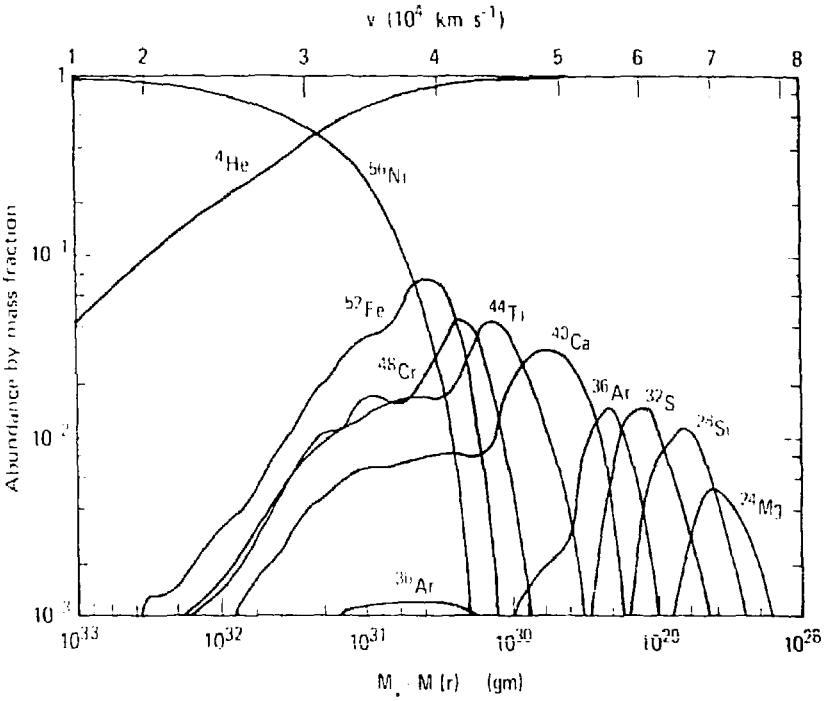
v (10^4 km s^{-1})
1
2
3
4
5
6
7
8
Abundance by mass fraction
1
10^{-1}
10^{-2}
10^{-3}
^{4}He
^{56}Ni
^{52}Fe
^{48}Cr
^{44}Ti
^{40}Ca
^{36}Ar
^{32}S
^{28}Si
^{24}Mg
^{30}Ar
10^{33}
10^{32}
10^{31}
10^{30}
10^{29}
10^{28}
$M_\odot$ M (r) (gm)

Figure 3

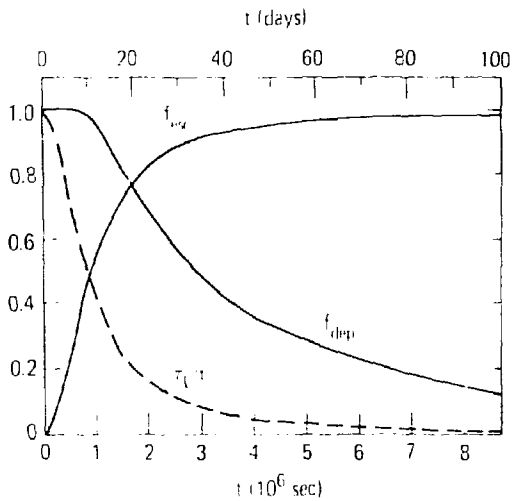

Figure 4

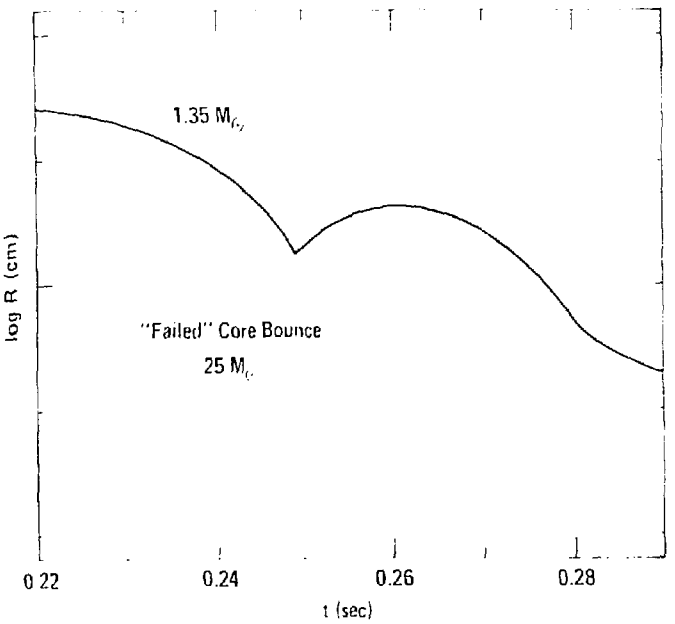

Figure 1

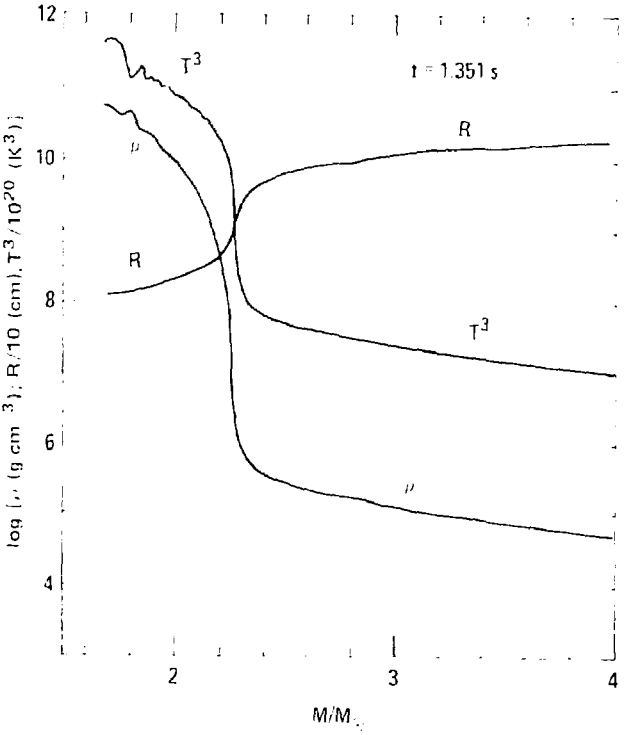

Figure 6

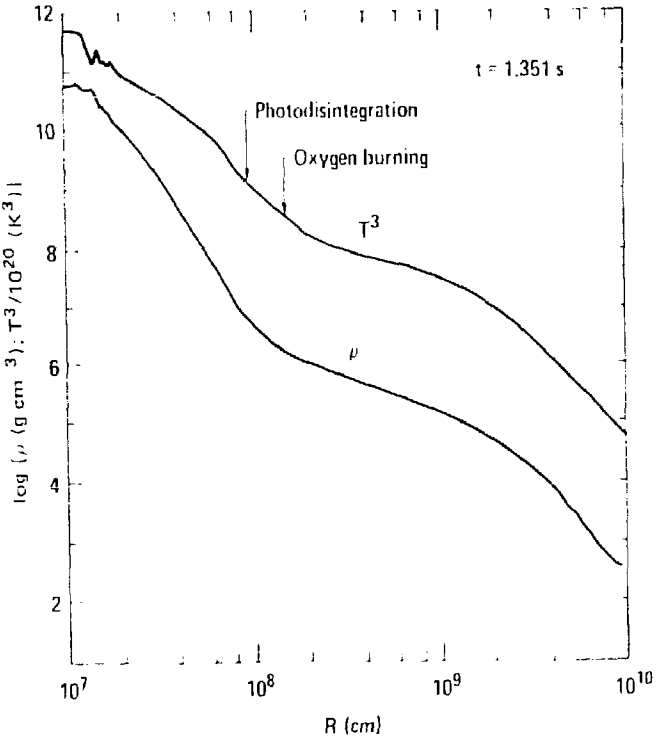
12
10
8
6
4
2
t = 1.351 s
Photodisintegration
Oxygen burning
T^3
ρ
log (ρ (g cm^{-3}); $T^3/10^{20}$ (K^3))
10^7
10^8
10^9
10^{10}
R (cm)

Figure 7

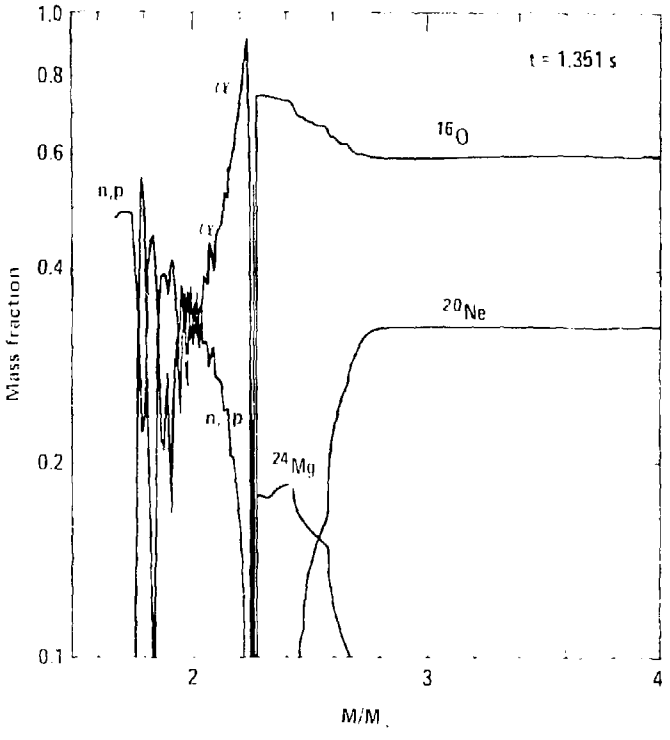
t = 1.351 s
^{16}O
^{20}Ne
^{24}Mg
n,p
Mass fraction
M/M$_\odot$
1.0
0.8
0.6
0.4
0.2
0.1
2
3
4

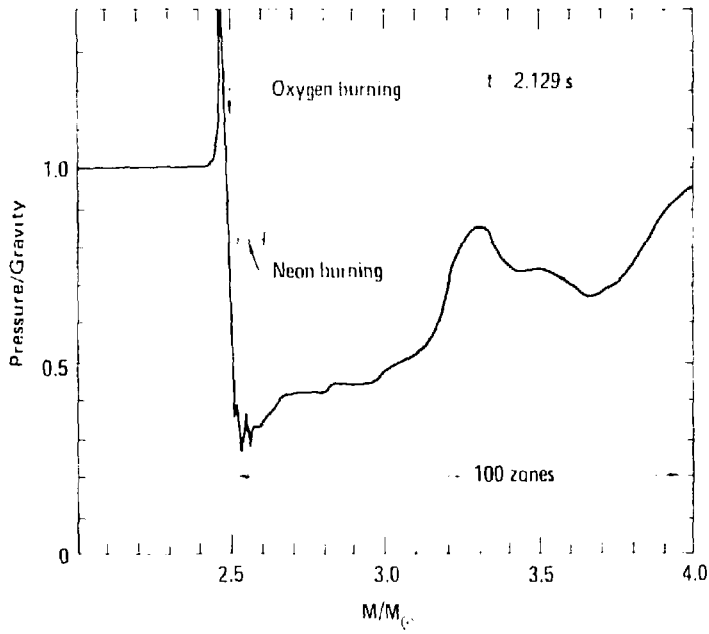
Oxygen burning
t 2.129 s
Neon burning
100 zones
Pressure/Gravity
1.0
0.5
0
2.5
3.0
3.5
4.0
M/M⊙

Figure 9

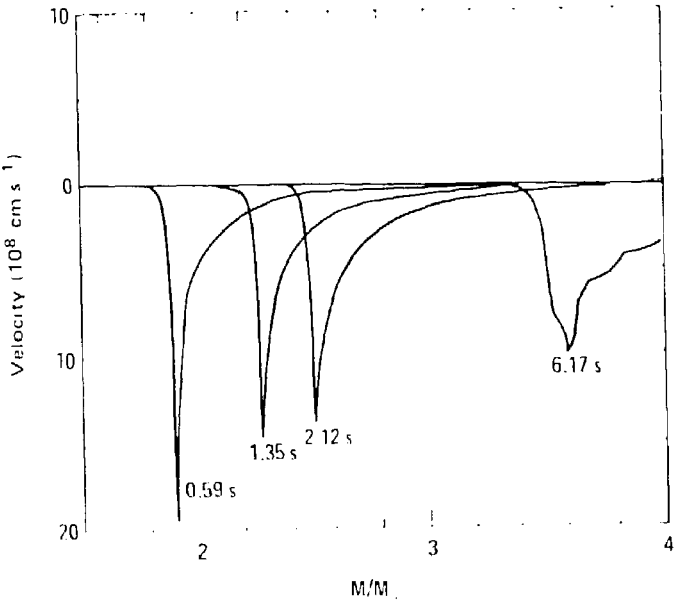

Figure 10

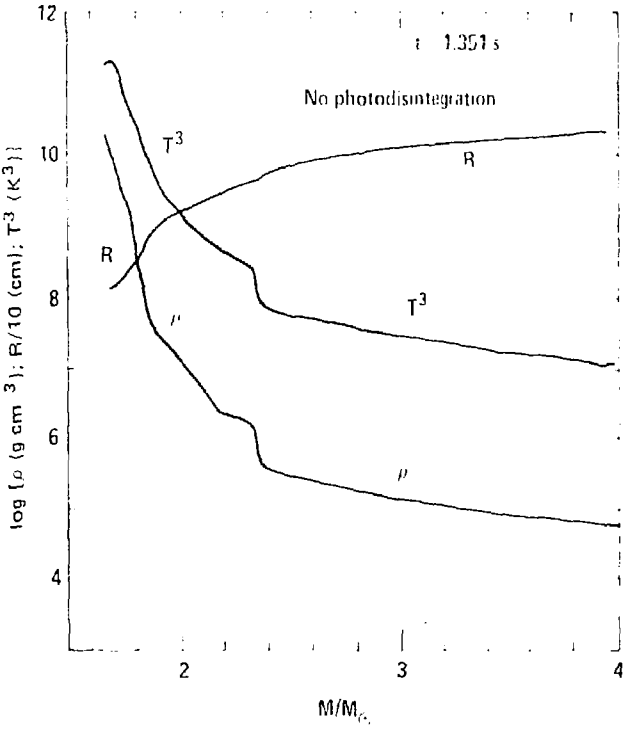
12
10
8
6
4
2
3
4
t = 1.351 s
No photodisintegration
T3
R
R
T3
ρ
ρ
log [ρ (g cm−3); R/10 (cm); T3 (K3)]
M/M⊙

Figure 11

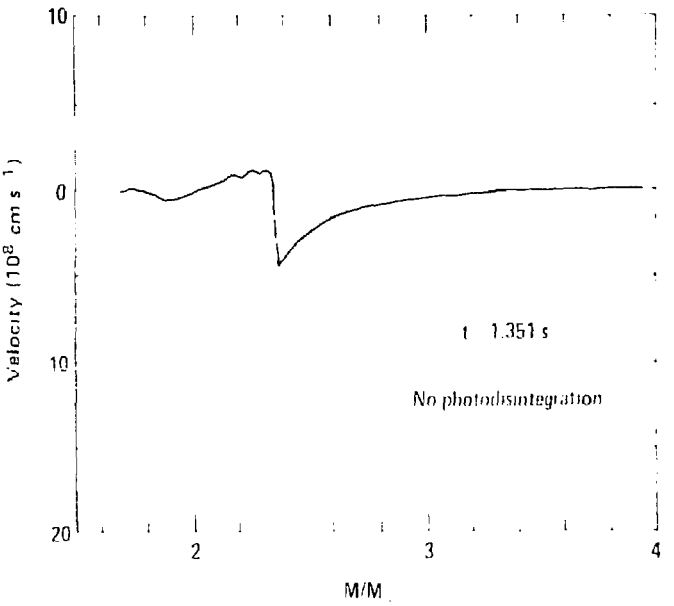
10
0
10
20
Velocity (10^8 cm s^{-1})
t 1.351 s
No photodisintegration
2
3
4
M/M

Figure 12

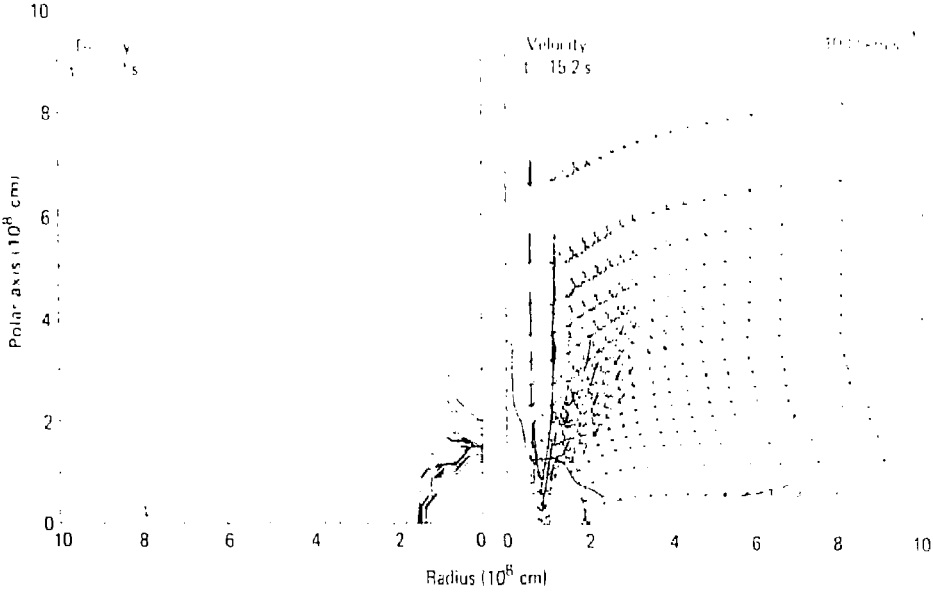
Velocity
t 15.2 s
Polar axis (10^8 cm)
Radius (10^8 cm)
10
8
6
4
2
0
0
2
4
6
8
10

Figure 1:

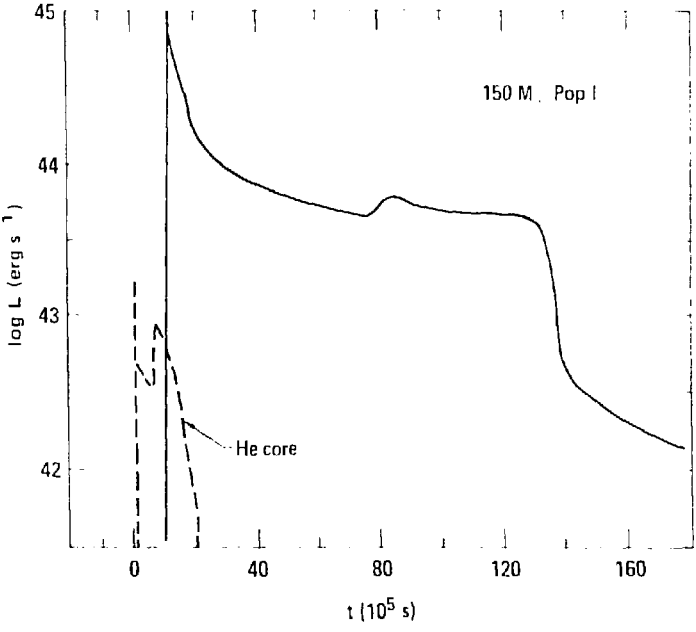

Figure 11

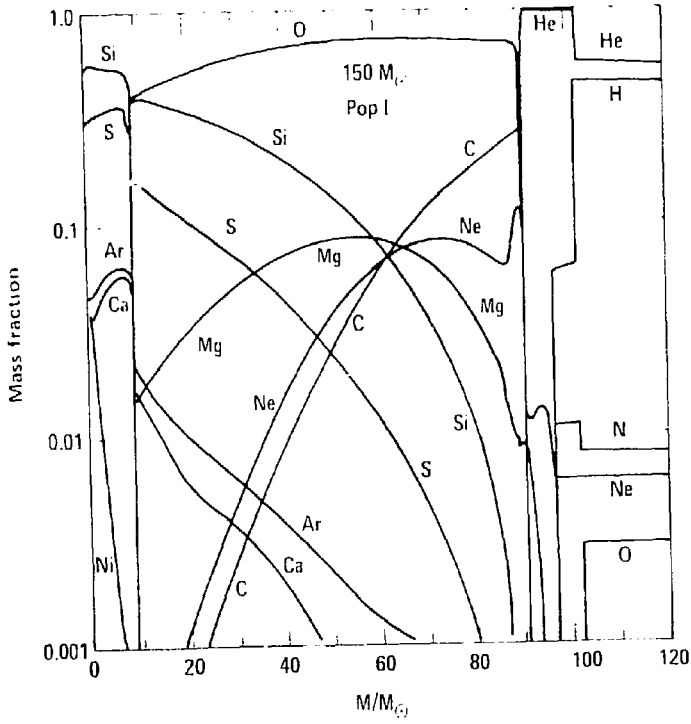
1.0
0.1
0.01
0.001
Mass fraction
0
20
40
60
80
100
120
M/M⊙
150 M⊙
Pop I
O
Si
S
Ar
Ca
Ni
Mg
Ne
C
He
H
N

Figure 15

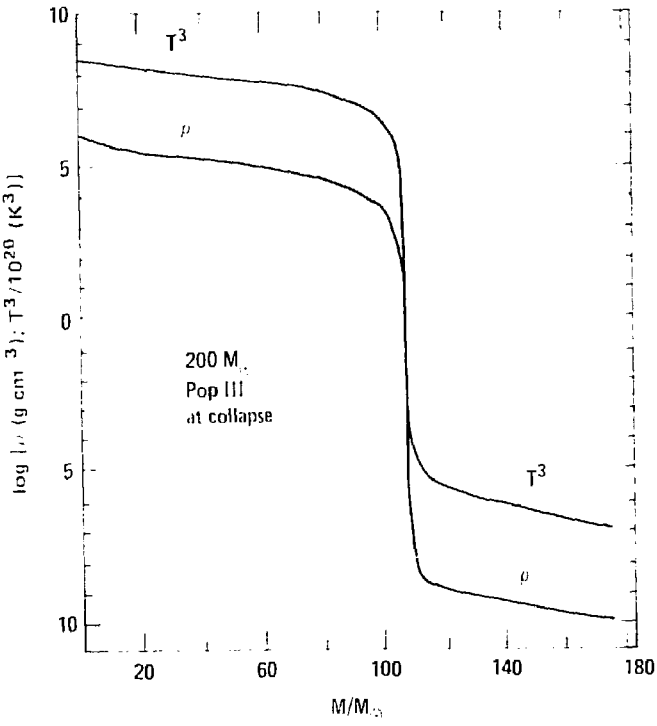
10
5
0
5
10
T3
ρ
200 M⊙
Pop III
at collapse
T3
ρ
20
60
100
140
180
M/M⊙
log [ρ (g cm⁻³); T³/10²⁰ (K³)]

Figure 1

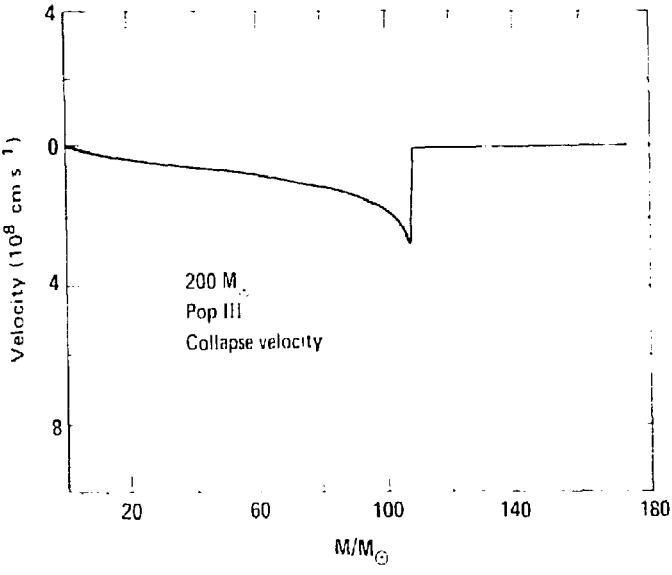
4
0
4
8
Velocity (10^8 cm s^{-1})
200 M$_\odot$
Pop III
Collapse velocity
20
60
100
140
180
M/M$_\odot$

Figure 17

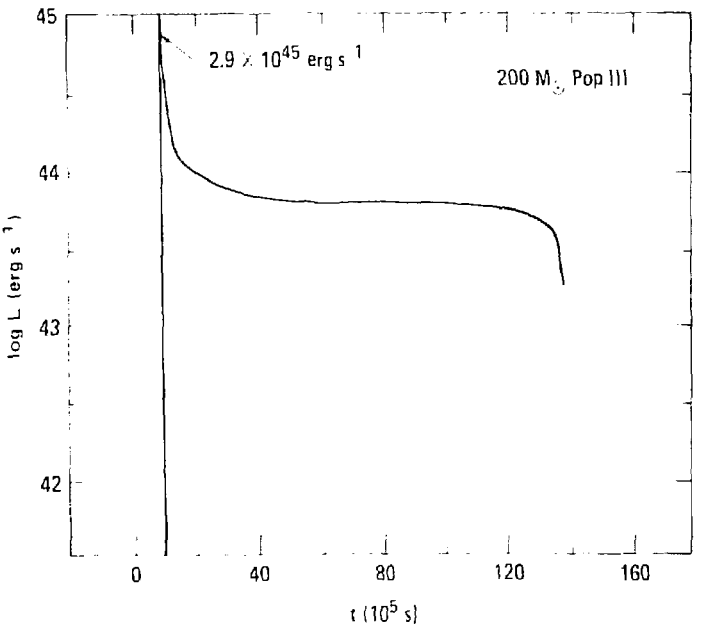
45
44
43
42
log L (erg s^{-1})
2.9 × 10^{45} erg s^{-1}
200 M$_\odot$ Pop III
0
40
80
120
160
t (10^5 s)

Figure 15

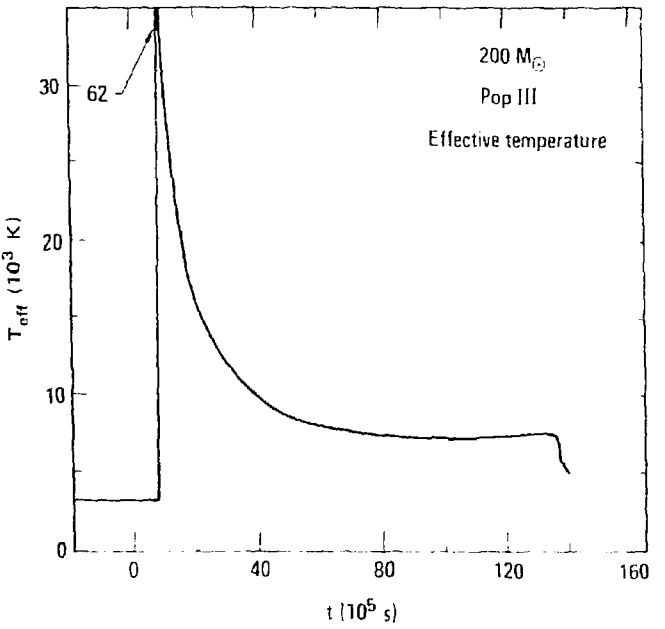
200 M⊙
Pop III
Effective temperature
62
30
20
10
0
T_{eff} (10^3 K)
0
40
80
120
160
t (10^5 s)

Figure 19

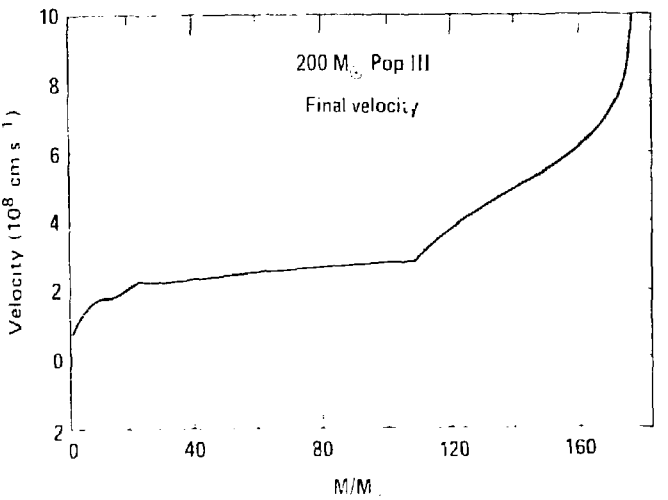
200 M⊙ Pop III
Final velocity
Velocity (10^8 cm s^{-1})
10
8
6
4
2
0
2
0
40
80
120
160
M/M⊙

Figure 16

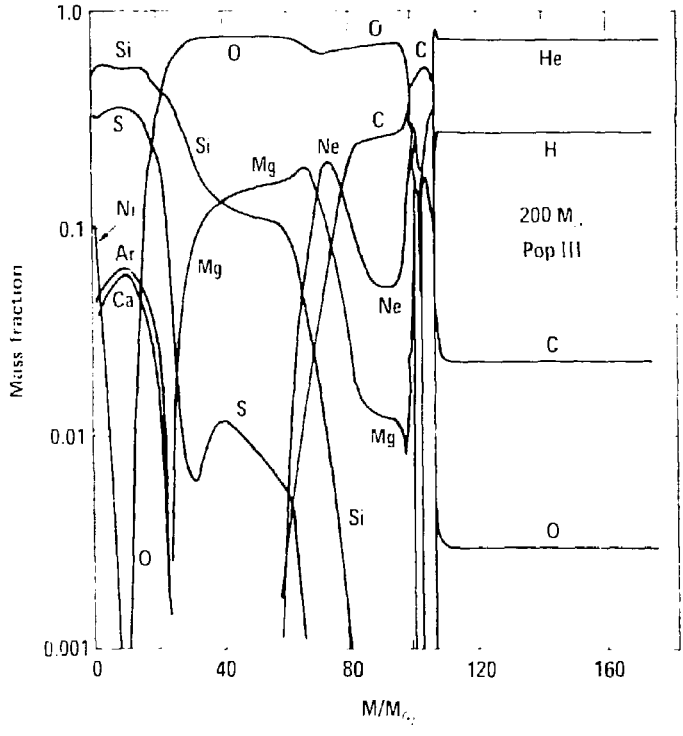
1.0
0.1
0.01
0.001
Mass fraction
0
40
80
120
160
M/M⊙
Si
O
O
C
He
S
Si
Mg
Ne
C
H
Ni
Ar
Ca
Mg
200 M⊙
Pop III
Ne
C
S
Mg
Si
O
O

Figure 11